PERFORMANCE ANALYSIS AND OPTIMIZATION OF MULTI-STAGE COMBINED THERMOELECTRIC GENERATORS

Fankai Meng[1, 2, 3], Lingen Chen[1, 2, 3*], Yuanli Feng [1, 2, 3] , Xiaowei Liu[1, 2, 3] and Tianchi Zhao[1, 2, 3]
*Author for correspondence
1 Institute of Thermal Science and Power Engineering, Naval University of Engineering, Wuhan 430033, China;
2 Military Key Laboratory for Naval Ship Power Engineering, Naval University of Engineering, Wuhan 430033, China;
3 College of Power Engineering, Naval University of Engineering, Wuhan 430033, China.
E-mail: lgchenna@yahoo.com; lingenchen@hotmail.com

ABSTRACT

A numerical model of multi-stage combined thermoelectric generators is established based on non-equilibrium thermodynamics. Taking a 5-stage thermoelectric generator for example, the output characteristics are analyzed. With the power and efficiency as the goal, the thermoelectric elements configuration and electrical current are optimized synchronously. The results show that when the temperature difference and the Seebeck coefficient are small, same number of thermoelectric elements in each stage results in the maximal power output; when the temperature difference or the Seebeck coefficient is large, the optimal configuration is that the numbers of thermoelectric elements increase with the same difference from the high temperature stage to the low temperature stage.

INTRODUCTION

Over the past decades, thermoelectric devices have become competitive solutions for waste heat recovery and cooling applications [1]. In order to obtain the actual characteristics of thermoelectric devices, various irreversible factors need to be taken into account. Finite time thermodynamics (FTT) [2-4] is an extension of classical thermodynamics and a new branch of modern thermodynamics. It has been widely used in many fields, such as physics, chemistry and engineering thermophysics. Based on this theory, many scholars have studied the performance of various types of thermoelectric devices. Sahin and Yilbas [5] formulated influence of thermoelectric leg geometry on generation efficiency. Meng et al. [6,7] and Chen et al. [8] investigated the performance of a combined thermoelectric refrigerator and presented a thermoelectric waste heat utilization solution recycling wastewater heat [8].

In order to get a larger temperature difference (TD) and lower temperature, a two-stage or multi-stage thermoelectric cooler is used. Study on the cascade thermoelectric cooler has been a hot spot in the research of thermoelectric refrigeration. Hu et al [9], Wang et al [10], Xuan et al. [11], Sharma et al. [12], Kaushik and Manikandan [13] investigated the cooling capacity and COP of two-stage and multi-stage thermoelectric refrigerator.

NOMENCLATURE

I	[A]	Electric current
K	[W/K]	Thermal conductance
M	[-]	Total number of thermoelectric element
m	[-]	Number of thermoelectric element of some stage
P	[W]	Power output
Q	[W]	Rate of heat flow
R	[Ω]	Electric resistance
r	[-]	Load resistance ratio
T	[K]	Temperature
TD	[K]	Temperature difference
U	[V]	Voltage

Special characters

α	Seebeck coefficient of thermoelectric element
η	Efficiency

Subscripts

c	Cold junction
h	Hot junction
L	Load
max	Maximum
M	Open circuit
max	Short circuit
0	Ambient or reference

Superscripts

P For maximum power
η For maximum efficiency

The considered factors include cross-sectional area ratio, length ratio of semiconductor legs, the optimal current, and thermal resistance of heat sink, and so on.

Also, to expand the sustainable temperature difference, multi-stage thermoelectric generators are applied as shown in Figure 1. The cold junction of the upper stage is the hot junction of the next stage. The total TD of the device is the superposition of the TD at each stage. There are some researches on the two stage thermoelectric generator. Liang et al. [14] Liu C et al.[15], Arora et al. [16] Manikandan and Kaushik [17] found that the thermocouple ratio between the two stage is important factor. The thermal efficiency is improved compared to single-stage thermoelectric generator.

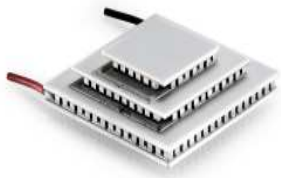

Figure 1 A multi-stage combined thermoelectric generator

However, researches on multi-stage thermoelectric generator have not been seen in public reports. The purpose of this paper is solving the problem that how to determine the optimal current and how to construct a high performance multi-stage thermoelectric generator with finite thermoelectric elements.

MODELING AND SOLUTION PROCEDURE

A model of multi-stage combined thermoelectric generators is shown in Figure 2. The device contains a total number of M thermoelectric elements. There are m_i thermoelectric elements in stage i, respectively. T_h and T_c represent the top stage temperature and the bottom stage temperature, respectively. The temperatures of the junctions between the two stages are T_i, $(1 \le i \le n-1)$ from the high temperature stage to the low temperature stage, respectively. The absorbed and rejected heat flow rates are Q_h and Q_c. Heat flow rates of the inter-stage are Q_i $(1 \le i \le n-1)$. The load resistance and electric current are R_L and I, respectively. The Joulean heat loss is I^2R and heat conduction loss is $K\Delta T_i$ of a thermoelectric element in each stage, where ΔT_i is the TD of stage i.

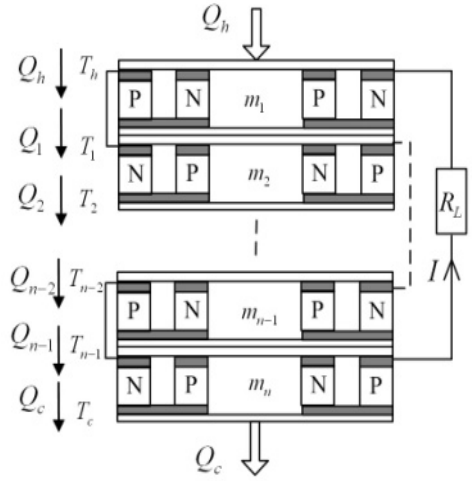

Figure 2 A model of a multi-stage combined thermoelectric generator

Based on the non-equilibrium thermodynamics, one can obtain:

$$Q_h = m_1[\alpha I T_h + K(T_h - T_1) - 0.5I^2R] \quad (1)$$

$$\begin{aligned} Q_1 &= m_1[\alpha I T_1 + K(T_h - T_1) + 0.5I^2R] \\ &= m_2[\alpha I T_1 + K(T_1 - T_2) - 0.5I^2R] \end{aligned} \quad (2)$$

$$\begin{aligned} Q_i &= m_i[\alpha I T_i + K(T_{i-1} - T_i) + 0.5I^2R] \\ &= m_{i+1}[\alpha I T_i + K(T_i - T_{i+1}) - 0.5I^2R] \end{aligned} \quad (2 \le i \le n-2) \quad (3)$$

$$\begin{aligned} Q_{n-1} &= m_{n-1}[\alpha I T_{n-1} + K(T_{n-2} - T_{n-1}) + 0.5I^2R] \\ &= m_n[\alpha I T_{n-1} + K(T_{n-1} - T_c) - 0.5I^2R] \end{aligned} \quad (4)$$

$$Q_c = m_n[\alpha I T_c + K(T_{n-1} - T_c) + 0.5I^2R] \quad (5)$$

where $\alpha = \alpha_P - \alpha_N$. R and K represent the resistance and thermal conductance, respectively. K and R can be calculated by

$$K = 2kA/L, \quad R = 2L\rho/A \quad (6)$$

where k, ρ, A, L are the thermal conductivity, electrical resistivity, cross section area and length of the the semiconductor leg.

Eqs. (2)-(4) can be rearranged as a equations set consisting of $n-1$ equations about the unknown inter-stage temperatures T_i $(1 \le i \le n-1)$:

$$\frac{K_1}{m_1 K} T_1 + \frac{m_2}{m_1} T_2 = -T_h - \frac{0.5 I^2 R(m_1 + m_2)}{m_1 K} \tag{7}$$

$$T_{i-1} + \frac{K_i}{m_i K} T_i + \frac{m_{i+1}}{m_i} T_{i+1} = -\frac{0.5 I^2 R(m_i + m_{i+1})}{m_i K} \quad (2 \le i \le n-2) \tag{8}$$

$$T_{n-2} + \frac{K_{n-1}}{m_{n-1} K} T_{n-1} = -\frac{m_n}{m_{n-1}} T_c - \frac{0.5 I^2 R(m_{n-1} + m_n)}{m_{n-1} K} \tag{9}$$

where $K_i = \alpha I(m_i - m_{i+1}) - K(m_i + m_{i+1})$.

The temperatures of each inter-stage $T_i (1 \le i \le n-1)$ can be obtained by solving Eq. (7)-(9). Submitting T_i into Eq. (1)-(5) yields the heat flow rate through the inter-stages, and then the power from each stages

$$P_1 = Q_h - Q_1,\ P_i = Q_{i-1} - Q_i \quad (2 \le i \le n-1),\ P_n = Q_{n-1} - Q_c \tag{10}$$

The efficiencies of each stage are

$$\eta_1 = P_1 / Q_h,\ \eta_i = P_i / Q_{i-1}\ (2 \le i \le n-1),\ \eta_n = P_n / Q_{n-1} \tag{11}$$

The total power of the combined generator is

$$P = \sum_{i=1}^{n} P_i = Q_h - Q_c \tag{12}$$

The total efficiency of the combined generator is

$$\eta = P / Q_h \tag{13}$$

OUTPUT CHARACTERISTICS ANALYSIS

To analyze the output characteristics of multi-stage combined thermoelectric generators, a 5-stage combined thermoelectric generator with same number of thermoelectric element in each stage ($m_i = M/5 \quad (1 \le i \le 5)$) is analyzed as an example. In the calculations, $\alpha = 4 \times 10^{-4} V/K$, $K = 0.03 W/K$, $R = 0.002\Omega$, $M = 120$, $T_h = 600K$, and $T_c = 300K$ ($\Delta T = 300K$) are set.

Figures 3 and 4 show the current output and voltage output versus the load resistance ratio r_L (the ratio of load resistance to the total internal resistance). It can be seen that with the increase of load resistance ratio, the electric voltage increases while the electric current decreases. When $r_L \to 0$, the voltage tends to the short circuit voltage $U_{short} = 0$, while the electric current tends to the short circuit current $I_{short} = 4.8A$; when $r_L \to \infty$, the voltage tends to the short circuit voltage $U_{open} = 2.6V$, while the electric current tends to the short circuit current $I_{short} = 0$.

Figure 5 shows the total power and total efficiency versus the current. It is found that there are two different optimal currents I^P and I^η corresponding to the maximum power $P_{\max}$ and the maximum efficiency $\eta_{\max}$, respectively. The relative magnitude of the two optimal currents is $I^P > I^\eta$. This characteristic is similar to a single-stage thermoelectric generator.

Due to that both power and efficiency should be considered in the design, the current should conform to $I^\eta < I < I^P$. Figure 6 shows the relation between power and efficiency. It is found that the curve is narrow twisted. The operating region between the two optimum points is small. The operating regions of the device should be:

$$P^\eta < P < P_{\max},\ \eta^P < \eta < \eta_{\max} \tag{14}$$

where $P_{\max}$ and $\eta_{\max}$ represent the maximum power and maximum efficiency, η^P and P^η represent the corresponding efficiency and power.

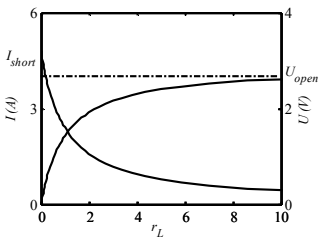

Figure 3 Output voltage and electric current versus load resistance ratio

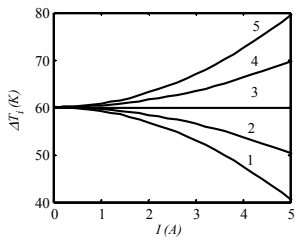

Figure 4 Temperature differences of each stage versus output current

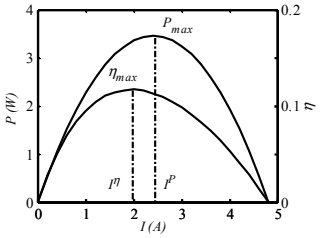

Figure 5 Power and efficiency versus current

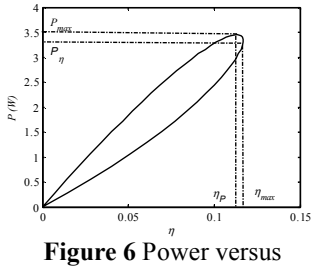

Figure 6 Power versus efficiency

Numerical simulation also shows that for given total working TD and output current, the TD in each stage is with the same difference; the power and efficiency increase in turn from the top to the bottom. There is a maximum current $I_{\max}$, so that there are powers from each stage. If $I > I_{\max}$, there are one or more stages consume power. This is an important

characteristic that distinguishes a multi-stage thermoelectric generator from a simple single-stage thermoelectric generator.

PERFORMANCE OPTIMIZATION

Above analyses are based on a multi-stage combined thermoelectric generator with same number in each stage. Then what is the optimal number of optimal thermoelectric elements in each stage and what is the optimal electric current are other interesting and important problems. In this section, the power and efficiency are optimized. The effects of working TD and the Seebeck coefficient will be analyzed, respectively. $n=5$, $M=1000$ are set in the optimization. m_i $(1<i<5)$ and I are set as design variables.

The optimization objectives are set as follows

$$\max\ P(m_1,m_2,m_3,m_4,m_5,I) \tag{15}$$

$$\max\ \eta(m_1,m_2,m_3,m_4,m_5,I) \tag{16}$$

The optimization variables vector is

$$V=[m_1\ m_2\ m_3\ m_4\ m_5\ I] \tag{17}$$

The lower bound and upper bound are

$$lb=[1\ 1\ 1\ 1\ 1\ 0] \tag{18}$$

$$ub=[M\ M\ M\ M\ M\ \inf] \tag{19}$$

The linear equalities is

$$\sum_{i=1}^{5} m_i = M \tag{20}$$

In addition, there is integral constraint i.e. m_i is integer.

The numerical optimizations show that same number of thermoelectric elements in each stage, i.e. $m_i=m_{i+1}=M/n$ $(1\le i\le n-1)$, can obtain maximum efficiency. For a thermoelectric generator, power is more important than efficiency usually, so the power optimization is more important. Following contents are the optimization of power. The maximum efficiency and the corresponding current are also given for comparison.

Effect of working temperature difference

Figure 7 shows the optimal thermoelectric element configuration versus working TD at maximum power. It can be found that when the TD is less than $200K$, the optimal configuration is the same number in each stage; when the TD is more than $200K$, the optimal configuration is that the numbers of thermoelectric elements increase with the same difference from the top to the bottom stage, i.e. $\Delta m=m_{i+1}-m_i$ $(1\le i\le n-2)$ is a constant. With the increase of TD ΔT, the difference of number Δm increases. Thermoelectric materials with outstanding performance at high temperature have been discovered more and more, so the thermoelectric elements number optimization become more and more important.

Figure 8 shows the maximum power $P_{\max}$ and the corresponding efficiency η_P, the maximum efficiency $\eta_{\max}$ and the corresponding power P_η versus the temperature difference. $P_{\max}$, η_P, $\eta_{\max}$ and P_η increase with the temperature difference. However, the rates of slope of the four curves are different. When $\Delta T\to 0$, $\Delta P=P_{\max}-P^\eta\to 0$, $\Delta\eta=\eta_{\max}-\eta_P\to 0$. The rate of slope of $P_{\max}$ and P_η increase while the rate of slope of $\eta_{\max}$ and η_P curve decrease.

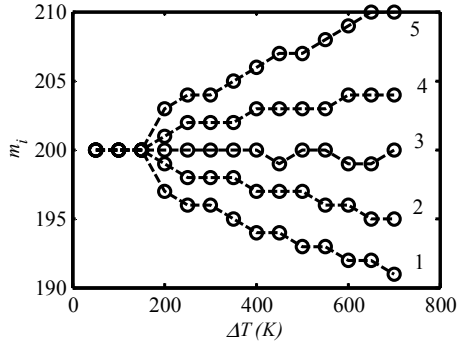

Figure 7 Optimal configuration of thermoelectric elements versus TD at maximum power

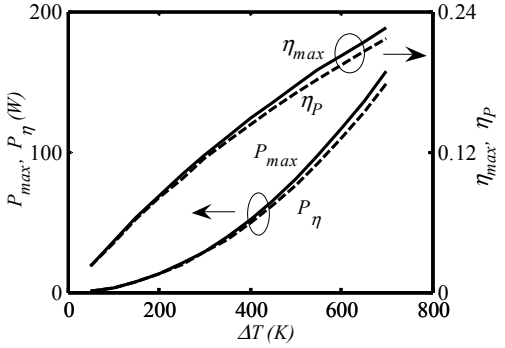

Figure 8 Maximum power and maximum efficiency versus TD

Effect of the Seebeck coefficient

Figure 9 shows the optimal thermoelectric element configuration versus the Seebeck coefficient at maximum power. It can be seen that for maximum power, when $\alpha<2\times10^{-4}V/K$, the optimal number of thermoelectric element of each stage is same; when the Seebeck coefficient is large, the optimal configuration is that the numbers of thermoelectric elements increase with the same difference from the top to the bottom stage, i.e. $\Delta m=m_{i+1}-m_i=$ $(1\le i\le n-2)$ is a constant. With the increase of Seebeck coefficient, the

difference of number of thermoelectric elements among each stage Δm increases. New classes of thermoelectric materials with high Seebeck coefficient have been discovered in last years [18, 19], so the optimization of thermoelectric elements configuration is more and more important.

Figure 10 shows the maximum power and the corresponding efficiency, and maximum efficiency and the corresponding power versus the Seebeck coefficient. With the increase of the Seebeck coefficient, $P_{\max}$, η_P , $\eta_{\max}$ and P_η increase. The change features of the four curves are similar to the curves versus the working TD

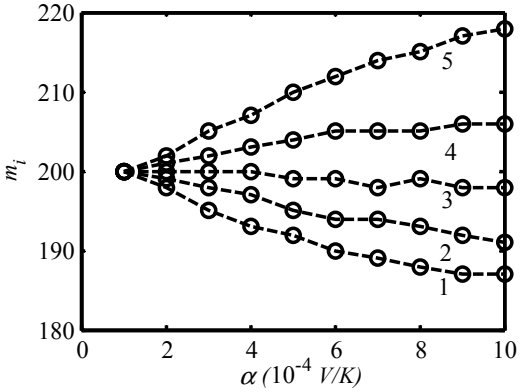

Figure 9 Optimal configuration of thermoelectric elements versus Seebeck coefficient at maximum power

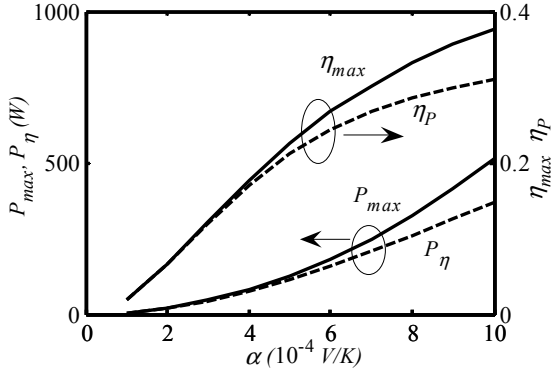

Figure 10 Maximum power and maximum efficiency versus Seebeck coefficient

Numerical simulation also shows that both open-circuit voltage and short-circuit current increase linearly approximately with the increase of TD and Seebeck coefficient.

The test platform of thermoelectric power generation has been set up. However, thermocouples of multi-stage thermoelectric generator bought from the market are fixed. The experiment is not yet available. In the future, we will communicate with manufacturers and make customized multi-stage thermoelectric products and then the experimental research will be carried out.

CONCLUSION

A model of multi-stage combined thermoelectric generators is established. The output characteristics are analyzed including the temperature differences, powers, and efficiencies of each stage, the total power and total efficiency. The thermoelectric elements configuration and output electric current are optimized, respectively. The major results are as follows:

(1) There are two different optimal currents corresponding to the maximum power and the maximum efficiency, respectively. This characteristic is similar to that of a single-stage thermoelectric generator.

(2) The working TD and the Seebeck coefficient affect the optimization variables strongly. When the TD and the Seebeck coefficient are small, same number of thermoelectric elements in each stage can obtain the maximum power; when the TD or the Seebeck coefficient is large, the optimal configuration is that the numbers of thermoelectric elements increase with the same difference from the top to the bottom stage.

(3) The maximum power increases accelerate while the maximum efficiency increases decelerate with the TD and Seebeck coefficient.

The conclusions obtained in this paper may provide some guidelines for the design of multi-stage thermoelectric generators.

ACKNOWLEDGEMENTS

This paper is supported by the National Nature Science Foundation of China (No. 11305266), the National Nature Science Foundation of China (No. 51576207) and Nature Science Foundation of Naval University of Engineering (No. 20161505). The authors wish to thank the reviewers for their careful, unbiased and constructive suggestions, which led to this revised manuscript.

REFERENCES

[1] Chen L.G., Meng F.K. and Sun F.R., Thermodynamic

analyses and optimization for thermoelectric devices_ The state of the arts. *Science China: Technological Sciences*, Vol.59, 2016, pp. 442-455

[2] Hoffmann K.H., Andresen B. and Salamon P., Finite-time thermodynamics tools to analyze dissipative processes. 2014: John Wiley & Sons.

[3] Ahmadi M.H., Ahmadi M.A. and Sadatsakkak S.A., Thermodynamic analysis and performance optimization of irreversible Carnot refrigerator by using multi-objective evolutionary algorithms (MOEAs). *Renewable and Sustainable Energy Reviews*, Vol.51, 2015, pp. 1055-1070

[4] Ge Y.L., Chen L.G. and Sun F.R., Progress in finite time thermodynamic studies for internal combustion engine cycles. *Entropy*, Vol.18, 2016, pp. 139

[5] Sahin A.Z. and Yilbas B.S., The thermoelement as thermoelectric power generator: Effect of leg geometry on the efficiency and power generation. *Energy Conversion and Management*, Vol.65, 2013, pp. 26-32

[6] Meng F.K., Chen L.G. and Sun F.R., Performance optimization for two-stage thermoelectric refrigerator system driven by two-stage thermoelectric generator. *Cryogenics*, Vol.49, 2009, pp. 57-65

[7] Meng F.K., Chen L.G., Sun F.R. and Yang B., Thermoelectric power generation driven by blast furnace slag flushing water. *Energy*, Vol.66, 2014, pp. 965-972

[8] Chen L.G., Meng F.K. and Sun F.R., Effect of heat transfer on the performance of thermoelectric generator-driven thermoelectric refrigerator system. *Cryogenics*, Vol.52, 2012, pp. 58-65

[9] Hu H.M., Ge T.S., Dai Y.J. and Wang R.Z., Experimental investigation on two-stage thermoelectric cooling system adopted in isoelectric focusing. *International Journal of Refrigeration*, Vol.53, 2015, pp. 1-12

[10] Wang T., Wang Q., Leng C. and Wang X., Parameter analysis and optimal design for two-stage thermoelectric cooler. *Applied Energy*, Vol.154, 2015, pp. 1-12

[11] Xuan X.C., Optimum staging of multistage exo-reversible refrigeration systems. *Cryogenics*, Vol.43, 2003, pp. 117-124

[12] Sharma S., Dwivedi V.K. and Pandit S.N., Exergy analysis of single-stage and multi stage thermoelectric cooler. *International Journal of Energy Research*, Vol.38, 2014, pp. 213-222

[13] Kaushik S.C. and Manikandan S., The influence of Thomson effect in the performance optimization of a two stage thermoelectric cooler. *Cryogenics*, Vol.72, 2015, pp. 57-64

[14] Liang X., Sun X., Tian H., Shu G., Wang Y. and Wang X., Comparison and parameter optimization of a two-stage thermoelectric generator using high temperature exhaust of internal combustion engine. *Applied Energy*, Vol.130, 2014, pp. 190-199

[15] Liu C., Pan X., Zheng X., Yan Y. and Li W., An experimental study of a novel prototype for two-stage thermoelectric generator from vehicle exhaust. *Journal of the Energy Institute*, Vol.89, 2016, pp. 271-281

[16] Arora R., Kaushik S.C. and Arora R., Multi-objective and multi-parameter optimization of two-stage thermoelectric generator in electrically series and parallel configurations through NSGA-II. *Energy*, Vol.91, 2015, pp. 242-254

[17] Manikandan S. and Kaushik S.C., The influence of Thomson effect in the performance optimization of a two stage thermoelectric generator. *Energy*, Vol.100, 2016, pp. 227-237

[18] Meroz O., Ben-Ayoun D., Beeri O. and Gelbstein Y., Development of Bi2Te2.4Se0.6 alloy for thermoelectric power generation applications. *Journal of Alloys and Compounds*, Vol.679, 2016, pp. 196-201

[19] So K.P., Chen D., Kushima A., Li M., Kim S., Yang Y., Wang Z., Park J.G., Lee Y.H., Gonzalez R.I., Kiwi M., Bringa E.M., Shao L. and Li J., Dispersion of carbon nanotubes in aluminum improves radiation resistance. *Nano Energy*, Vol.22, 2016, pp. 319-327